JCB Article

Characterization of a mammalian Golgi-localized protein complex, COG, that is required for normal Golgi morphology and function

Daniel Ungar,[1] Toshihiko Oka,[2] Elizabeth E. Brittle,[1] Eliza Vasile,[2,3] Vladimir V. Lupashin,[4] Jon E. Chatterton,[2] John E. Heuser,[5] Monty Krieger,[2] and M. Gerard Waters[1]

[1]Department of Molecular Biology, Princeton University, Princeton, NJ 08544
[2]Department of Biology, Massachusetts Institute of Technology, Cambridge, MA 02139
[3]Departments of Pathology, Beth Israel Deaconess Medical Center, Boston, MA 02215
[4]Department of Physiology and Biophysics, University of Arkansas for Medical Sciences, Little Rock, AR 72205
[5]Department of Cell Biology and Physiology, Washington University School of Medicine, St. Louis, MO 63130

Multiprotein complexes are key determinants of Golgi apparatus structure and its capacity for intracellular transport and glycoprotein modification. Three complexes that have previously been partially characterized include (a) the Golgi transport complex (GTC), identified in an in vitro membrane transport assay, (b) the ldlCp complex, identified in analyses of CHO cell mutants with defects in Golgi-associated glycosylation reactions, and (c) the mammalian Sec34 complex, identified by homology to yeast Sec34p, implicated in vesicular transport. We show that these three complexes are identical and rename them the conserved oligomeric Golgi (COG) complex. The COG complex comprises four previously characterized proteins (Cog1/ldlBp, Cog2/ldlCp, Cog3/Sec34, and Cog5/GTC-90), three homologues of yeast Sec34/35 complex subunits (Cog4, -6, and -8), and a previously unidentified Golgi-associated protein (Cog7). EM of ldlB and ldlC mutants established that COG is required for normal Golgi morphology. "Deep etch" EM of purified COG revealed an ~37-nm-long structure comprised of two similarly sized globular domains connected by smaller extensions. Consideration of biochemical and genetic data for mammalian COG and its yeast homologue suggests a model for the subunit distribution within this complex, which plays critical roles in Golgi structure and function.

Introduction

The eukaryotic secretory pathway consists of a set of membrane-bound compartments through which proteins move in transport vesicles or larger transport intermediates (Rothman, 1994). Vesicular transport from one compartment to the next can be divided into four sequential phases: vesicle budding; movement to the next compartment; association of the vesicle with the acceptor compartment; and fusion of vesicle and acceptor membranes (Rothman, 1994; Mellman and Warren, 2000). For the Golgi apparatus, the transport structures may be the Golgi cisternae themselves, as some secretory cargo moves through the Golgi without exiting the stack in vesicles (Bonfanti et al., 1998; Mironov et al., 2001).

Many Golgi proteins, such as glycosylation enzymes, are maintained in a nonuniform steady-state distribution through the cisternae. These proteins must be transported to their sites of residence and then either be retained there or, if they move beyond them, retrieved by retrograde vesicular transport (Harris and Waters, 1996; Martinez-Menarguez et al., 2001). Thus, all transport steps appear to involve the movement of small vesicles (either carrying cargo in the anterograde or resident enzymes in the retrograde direction) between larger membrane compartments (Pelham and Rothman, 2000).

Studies in yeast and mammalian cells have led to the identification of several multisubunit peripheral membrane protein complexes that are thought to be involved in membrane trafficking and/or compartment function, including the Sec6/8 (Grindstaff et al., 1998; Guo et al., 1999), the TRAPP I (Sacher et al., 2001), and the Sec34/35 (VanRheenen et al., 1998) complexes. The yeast Sec34/35 complex has

The online version of this article includes supplemental material.

Address correspondence to Monty Krieger, Biology Department, Massachusetts Institute of Technololgy, Room 68-483, 77 Massachusetts Ave., Cambridge, MA 02139. Tel.: (617) 253-6793. Fax: (617) 258-5851. E-mail: krieger@mit.edu

M. Krieger and M.G. Waters contributed equally to this work.

Key words: GTC-90 protein; ldlB protein; ldlC protein; Sec34 protein; Sec35 protein

eight subunits (Whyte and Munro, 2001), is localized to the Golgi apparatus (Spelbrink and Nothwehr, 1999; Kim et al., 2001), and has been suggested to be involved in anterograde ER to Golgi (VanRheenen et al., 1998; Kim et al., 2001), retrograde intra-Golgi (Ram et al., 2002), and endosome to Golgi (Spelbrink and Nothwehr, 1999) traffic. A mammalian Sec34-containing complex has also been identified and implicated in Golgi protein trafficking (Suvorova et al., 2001).

Another complex, called the Golgi transport complex (GTC),* was isolated because of its ability to stimulate an in vitro intra-Golgi transport assay (Walter et al., 1998). It is a hetero-oligomeric Golgi-localized complex of ~800 kD, comprising proteins between 70 and 110 kD. The 90-kD subunit of GTC, GTC-90, was identified and a cDNA encoding the protein was cloned.

The ldlCp complex was discovered during the analysis of low-density lipoprotein receptor (LDLR)–defective CHO cell mutants, ldlB and ldlC (Krieger et al., 1981; Podos et al., 1994; Chatterton et al., 1999). The ldlB- and ldlC-null mutants, which are viable, exhibit defects in multiple Golgi-associated reactions that result in the abnormal processing of the LDLR and many other glycoconjugates (Kingsley et al., 1986). The defects are not due to drastic disruptions in secretion or endocytosis (Kingsley et al., 1986; Reddy and Krieger, 1989). The ldlCp protein (~80 kD) is a component of a large peripheral Golgi complex whose size and Golgi-association are dependent on ldlBp (~110 kD) (Podos et al., 1994; Chatterton et al., 1999), which suggested that they are components of the same complex.

Similarities in the sizes, locations, and subunits of the ldlCp complex and GTC suggested that they might be identical (Chatterton et al., 1999). We have explored this possibility through identification of all the subunits of purified GTC and examination of the physical association of the proteins in tissues and wild-type and mutant cultured cells. We have found that GTC and the ldlCp complexes are the same, and it appears to be to the mammalian homologue of the yeast Sec34/35 complex. This is consistent with the report of Whyte and Munro (2001; which appeared during the preparation of this manuscript), which showed that the yeast homologue of GTC-90, Cod4p, is a subunit of the Sec34/35 complex. We suggest that this mammalian complex be called conserved oligomeric Golgi (COG) complex, and its subunits be designated Cog1–8. We have also examined by EM the structure of the COG complex and the effects of the null mutations in ldlB (Cog1) and ldlC (Cog2) on Golgi structure.

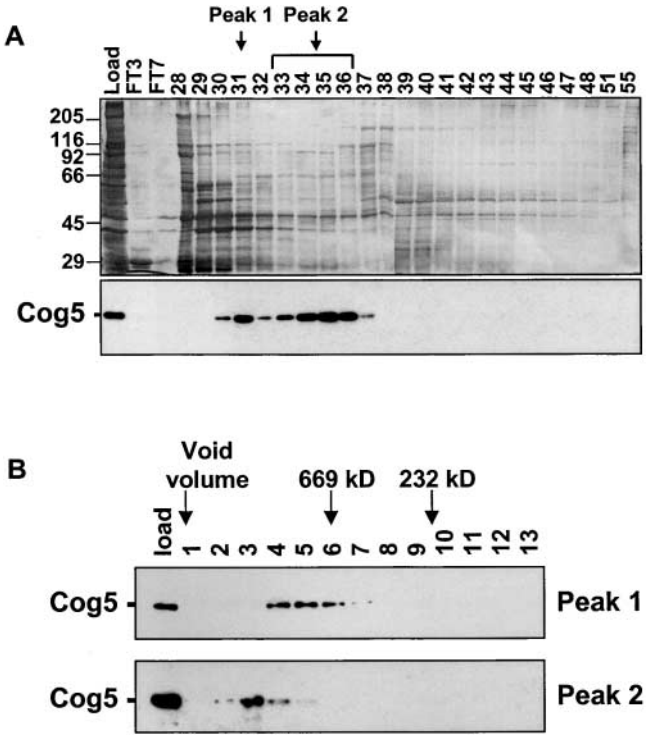

Figure 1. **Identification of two Cog5-containing protein complexes in bovine brain cytosol.** (A) Partially purified COG complex from bovine brain cytosol was subjected to ceramic hydroxyapatite chromatography (see Materials and methods). The eluted fractions were separated by 10% SDS-PAGE and either silver stained (top) or subjected to immunoblotting with anti-Cog5 antibody (bottom). "Load" is the sample before chromatography, and FT3 and FT7 are representative flow-through fractions; fractions 28–55 were collected during elution with a phosphate gradient. The positions of molecular weight markers (kD) are shown on the left. Peaks 1 and 2 represent Cog5-containing proteins eluting in fractions 31 and 33–36, respectively. (B) Peak 1 (9% of fraction 31) and peak 2 (2% of the pooled fractions 33–36) from the chromatogram shown in A were subjected to gel filtration chromatography on a SMART Superose 6 column followed by 10% SDS-PAGE and immunoblotting with the anti-Cog5 antibody. Load is the sample before chromatography. The void volume and the elution positions of size standards (thyroglobulin, 669 kD; catalase, 232 kD) are shown at the top. All samples loaded onto gels and immunoblots represent equivalent amounts within a chromatogram.

Results

Improved COG complex purification

We modified the previously described (Walter et al., 1998) method of COG purification from bovine brain to improve the yield (Table I) and followed the purification by anti-Cog5 immunoblotting. During the purification, two peaks of Cog5 were resolved by hydroxyapatite chromatography (Fig. 1 A). Similar complexes were also seen in CHO cell lysates not subjected to the multiple purification steps (see Fig. 7 B). We purified the protein eluting in the second peak because it represented the larger complex (Fig. 1 B), here defined as COG. It is not clear if both complexes are present in vivo or if the small complex was generated during cell/tissue lysis, or if the peak 1 material, which is slightly smaller in size than COG (Fig. 1 B), shares COG components other than Cog5.

SDS-PAGE analysis of the fractions from the final purification step (Table I and Fig. 2) indicated that COG is composed of eight subunits. If one copy of each subunit were present in the complex, the calculated molecular weight would be 700 kD.

Identification of subunits of the mammalian COG complex

Purified COG subunits were excised from the SDS-PAGE gel individually (Cog1, -2, -6, and -8) or in pairs (Cog3/

*Abbreviations used in this paper: COG, conserved oligomeric Golgi; GTC, Golgi transport complex; HA, hemagglutinin; IB, immunoblotting; IF, immunofluorescence; LDLR, low-density lipoprotein receptor.

Table I. **COG complex purification protocol**

Purification step	Total protein	Yield of total protein	Yield of COG complex[a]
	mg	*%*	*mg*
Bovine brain	1.5×10^6	–	–
Bovine brain cytosol	40,000.0	100	ND
Ammonium sulfate	10,200	25.5	3.5
Butyl-Sepharose pool	1,080	2.7	2.1
MonoQ pool	43	0.11	0.63
Ceramic hydroxyapatite pool	3.3	0.082	0.28
Superose 6 pool	0.5	1.2×10^{-3}	ND
MiniQ pool	0.07	1.75×10^{-4}	0.07

[a]The yield of COG complex was estimated by quantification of anti-Cog5 immunoblots; the values for the steps before the ceramic hydroxyapatite pool are overestimates of the true yield of COG because of the copurification of a smaller Cog5-containing complex.

Cog5 and Cog4/Cog7) and sequenced by mass spectrometry. Eight protein components were identified (Table II and Fig. 2 B). All except Cog7 (see below) had been previously suggested to be components of various mammalian Golgi-associated complexes. The four individually excised proteins were identified: Cog1 as ldlBp; Cog2 as ldlCp; and Cog6 and -8 as the homologues of yeast Cod2p and Dor1p, respectively. One pair, Cog3/Cog5, was identified as the mammalian Sec34 and GTC-90; the other, Cog4/Cog7, was found to be the homologue of yeast Cod1p (Cog4) and a previously unidentified protein (Table II and Fig. 2 B). The individual bands in the Cog3/Cog5 doublet were identified as Sec34 and GTC-90 based on immunoblotting (unpublished data). The assignments of the bands in the Cog4/Cog7 doublet were based on the predicted molecular weights of their human homologues and will require verification. The presence of Cog1, -2, and -3 in addition to Cog5 in the purified material was confirmed by immunoblotting partially (Fig. 3) and completely (Fig. 2 A) purified fractions.

Although present in the COG complex, the Cog1, -2, and -3 subunits were not detected by immunoblotting in the smaller Cog5-containing complex (Fig. 3, fractions 30–32).

It is noteworthy that during the early stages of development of this new purification protocol, we did not include the hydroxyapatite purification step (unpublished data). This resulted in the copurification of COG and the Sec6/8 complex (Hsu et al., 1996), which suggests that they share many physicochemical characteristics. This may not have been fortuitous, as it has been proposed that the COG and the Sec6/8 complexes are related (Whyte and Munro, 2001).

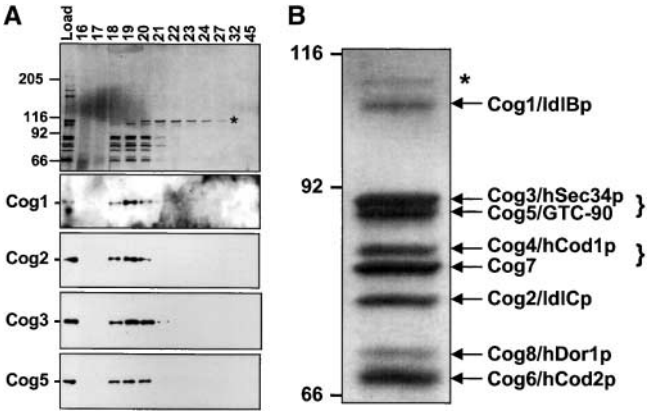

Figure 2. **MiniQ purification of COG and identification of its subunits.** (A) Peak 2 from the ceramic hydroxyapatite chromatogram in Fig. 1 A was further purified (Table I), and a portion of each fraction from the last chromatographic step (MiniQ) was subjected to 7.5% SDS-PAGE and silver staining (top; molecular weight markers [kD] shown on the left) or 10% SDS-PAGE and immunoblotting (bottom four panels) with antibodies to the indicated proteins. To resolve the individual bands, the 7.5% SDS-PAGE gel was run until proteins smaller than 60 kD ran off the gel. No additional components (or contaminants) were detected in the size range below 65 kD (verified by 15% SDS-PAGE; unpublished data). The load lane is the sample before chromatography. (B) Enlarged view of the lower portion of the lane containing fraction 19 in A. The indicated identities of the proteins were determined by mass spectrometry, as described in the text. The pairs marked by brackets were excised together and sequenced as a mixture. The protein marked with an asterisk is rabaptin-5, which is not part of the complex (A). The positions of molecular weight (kD) markers are shown on the left.

Cog7 is conserved in higher eukaryotes

The human Cog7 cDNA (GenBank/EMBL/DDBJ accession no. XM_041725) encodes a protein of 770 resi-

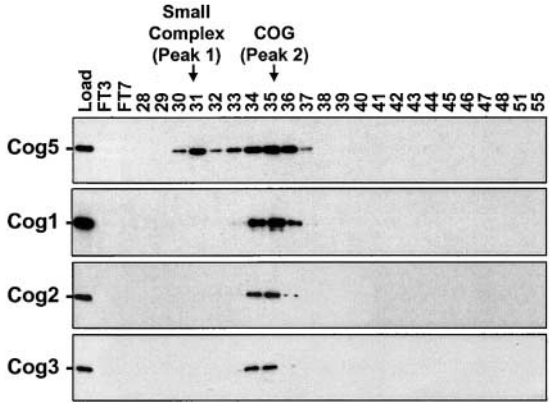

Figure 3. **Comparison of the subunit composition of the small and large Cog5-containing complexes.** Partially purified COG complex (purified by ammonium sulfate precipitation, butyl-Sepharose chromotography and MonoQ chromatography) was subjected to ceramic hydroxyapatite chromatography. Samples of the fractions were separated by 10% SDS-PAGE and subjected to immunoblotting with antibodies specific to the indicated proteins as described in the legend to Fig. 1 A. Labels are as in Fig. 1 A.

Table II. **Summary of COG complex subunits**

Subunit	Apparent mol wt (bovine)[g]	Calculated mol wt (human)[g]	Previously used mammalian nomenclature	*S. cerevisiae* homologue	
				Protein	ORF
Cog1	110	109	ldlBp[a]	(Cod3p/Sec36p)[f]	(YGL223c)[f]
Cog2	77	83	ldlCp[a]	(Sec35p)[f]	(YGR120c)[f]
Cog3	93	94	hSec34p[b]	Sec34p/Grd20p	YER157w
Cog4	84	89	hCod1p[d]	Cod1p/Sgf1p/Sec38p	YPR105c
Cog5	90	92	GTC-90[c]	Cod4p	YNL051w
Cog6	67	68	hCod2p[d]	Cod2p/Sec37p	YNL041c
Cog7	82	86	None[e]	(Cod5p)[f]	(YGL005c)[f]
Cog8	70	69	hDor1p[d]	Dor1p	YML071c

[a]Kingsley and Krieger, 1984.
[b]Suvorova et al., 2001.
[c]Walter et al., 1998.
[d]Whyte and Munro, 2001.
[e]GenBank/EMBL/DDBJ accession no. XP_041725.
[f]Very little or no sequence homology; however, for tentative assignments see text.
[g]In kD.

dues. Analysis of the human genome database (http://www.ncbi.nlm.nih.gov/genome/guide/human/) shows that the Cog7 gene is located on the short arm of chromosome 16 and contains 17 exons. The Paircoil algorithm (Berger et al., 1995) detected a potential coiled-coil domain between amino acids 70 and 100 of Cog7, however, the structure remains to be determined. Closely related homologues of Cog7 can be found in numerous vertebrates and invertebrates and several plants (Table III). However, homologues in *Caenorhabditis elegans* or *Saccharomyces cerevisiae* were not found. Thus, Cog7 joins Cog1 and Cog2 in having no obvious homologue in yeast. The functions of Cog1, -2, and -7 may be performed by other proteins in lower eukaryotes (see Discussion).

Cog1 and Cog7 are Golgi-associated proteins

We used immunofluorescence microscopy to locate endogenous Cog1 in CHO cells and Cog7 in HeLa cells transfected with an expression vector encoding a hemagglutinin (HA) epitope–tagged Cog7. Fig. 4 A shows that both Cog1 (top) and Cog7 (bottom) colocalized significantly, but not completely, with the Golgi marker mannosidase II in a perinuclear distribution. Similar results have been observed for Cog2 and Cog5 (Podos et al., 1994; Walter et al., 1998). Thus, like other COG complex components, Cog1 and Cog7 are Golgi associated.

Fig. 4 B shows double staining experiments in HeLa cells using antibodies to HA–Cog7 and Cog1, -3, and -5. These experiments show a high degree of colocalization of these four proteins, providing further evidence that they are components of a single complex.

Verification of the subunit composition of COG

Copurification of proteins provides strong, but not unequivocal, evidence that the proteins are members of a complex. Therefore, we performed coimmunoprecipitation experiments. COG from rat liver cytosol was immunoprecipitated (Fig. 5 A) using an anti-Cog2 antipeptide antibody (Podos et al., 1994) in the absence (lane 2) or presence (lane 3) of the immunogenic peptide to block the precipitation and subjected to SDS-PAGE and immunoblotting with antibodies to COG subunits. All of the COG subunits examined coprecipitated with Cog2 (lane 2) in an anti-Cog2 antibody-specific (compare lanes 1 and 2) and immunogenic peptide–inhibitable (lane 3) fashion. In each precipitation, ~10% or more of the total cytosolic content of each component (Fig. 5 A, lane 4) was recovered (lane 2). Similar results were observed using an anti-Cog1 monoclonal antibody to precipitate the complex from a partially purified sample of bovine brain cytosol (Fig. 5 B). As expected, the anti-Cog1 antibody did not precipitate Sec8, a component of the Sec6/8 complex (Hsu et al., 1996) (Fig. 5 B). Thus Cog1, -2, -3, and -5 are present in the same complex, and the GTC, ldlCp, and Sec34 complexes are the same entity.

COG architecture

The ultrastructure of purified COG was visualized by quick freeze/deep etch/rotary shadow EM (Heuser, 1983). The images in Fig. 6 are 3-D "anaglyphs," which are best viewed with red/green stereo glasses (Heuser, 2000). Samples that were prefixed with glutaraldehyde (Fig. 6, fixed) were compared with unfixed COG (Fig. 6, unfixed); glutaraldehyde fixation was used to preserve structures that might disassemble on contact with mica (Heuser, 1989). However, images of fixed samples must be interpreted with caution, as fixation can introduce structural artifacts due to cross-linking. Most of the images of the fixed samples and many of the un-

Table III. **Pair-wise sequence comparisons of the identities and similarities of Cog7 homologues**

	Human Cog7 (identity/similarity)	*Drosophila* Cog7 (identity/similarity)
	%	%
Drosophila Cog7	27/45	–
Arabidopsis Cog7	23/41	23/39

Percent identity and percent similarity were calculated using the GCG software package (Wisconsin package version 10.2). The GenBank/EMBL/DDBJ accession nos. for the human *Drosophila melanogaster* and *Arabidopsis thaliana* proteins are XP_041725, AAF56975, and BAB09754, respectively.

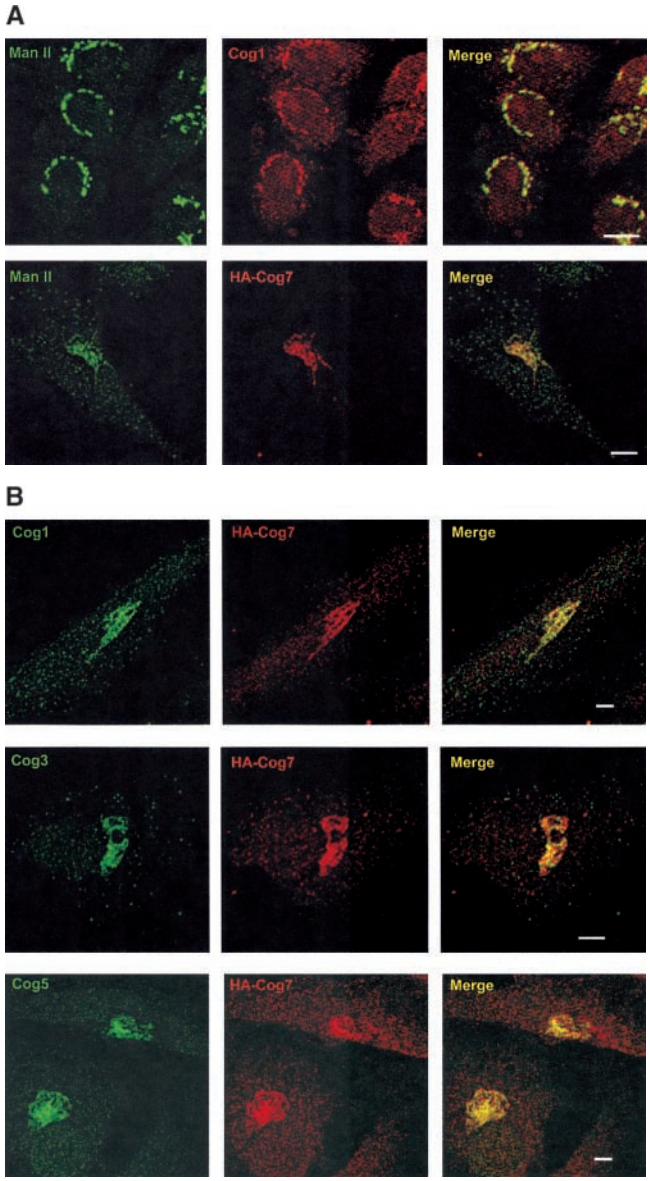

Figure 4. **Immunofluorescence localization of Cog1 and Cog7.** (A) CHO cells (top) or HeLa cells expressing HA epitope–tagged Cog7 (bottom) were fixed and double stained with primary antibodies to Cog1 or the HA epitope tag (HA–Cog7; center) and mannosidase II (Man II; left) and secondary antibodies labeled with either Alexa®488 (green)/Alexa®568 (red; top) or Alexa®488 (green)/Alexa®546 (red; bottom). Confocal microscopic images were collected and are displayed either as a field representing the distribution of a single antibody (left and center) or as the merged images (right). Bars, 10 μm. (B) HeLa cells expressing HA epitope–tagged Cog7 were fixed and double stained with primary antibodies to the indicated COG complex subunits and the HA epitope tag (HA–Cog7) and secondary antibodies labeled with either Alexa®488 (green) or Alexa®546 (red). Images are presented as in A.

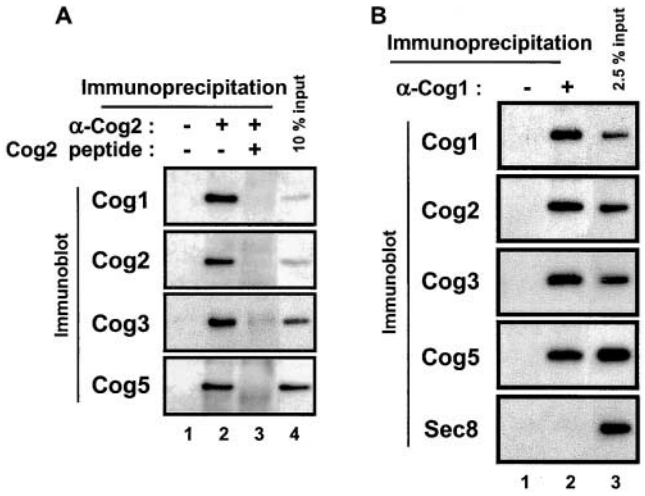

Figure 5. **Coimmunoprecipitation of COG complex subunits.** (A) Cog2 was immunoprecipitated from rat liver cytosol (lanes 2 and 3) with an anti-Cog2 antipeptide antibody in the absence (lane 2) or presence (lane 3) of the immunogenic peptide. The precipitates were fractionated by 6% SDS-PAGE and immunoblotted with the indicated antibodies. Lane 4 shows 10% of the starting cytosol sample. (B) Bovine brain COG complex, partially purified through the MonoQ chromatography step, was immunoprecipitated in the absence (lane 1) or presence (lane 2) of anti-Cog1 monoclonal antibody. The precipitates and 2.5% of the starting sample (lane 3) were fractionated by 6% SDS-PAGE and immunoblotted with antibodies to the indicated COG subunit or the Sec8 component of the mammalian Sec6/8 complex.

fixed samples suggest that COG is bilobed. In some images, the lobes appeared to be interconnected by thin rods and/or globules. The fixed form was 37 ± 4 (n = 18) nm long. Thus, COG appears to be slightly larger than the size marker thyroglobulin (670 kD; Fig. 6, leftmost in bottom row). The bilobed appearance of COG looks substantially different than comparable images of the mammalian Sec6/8 complex (Fig. 6, first four images in fifth row). The Sec6/8 complex appears to have a large globular or brick-shaped "core" that is surrounded by short extensions (Hsu et al., 1998). Other molecules suitable for comparison in size and shape with COG are shown in the bottom panels of Fig. 6 and are described in its legend.

About a third of the images of unfixed COG (Fig. 6, unfixed) appeared similar to the fixed samples, whereas the others appeared somewhat heterogeneous and "splayed." The splayed images tended to display two globules connected by disordered globular or rod-like connections. The splayed forms ranged up to 50–75 nm long. The overall size of this form was similar to that of a clathrin triskelion (Fig. 6, fourth image in row 5; Heuser and Kirchhausen, 1985). Presumably, such splayed forms represent COG complexes partially disassembled by adhesion with mica. Nevertheless, they illustrate that native COG seems to be a group of globular domains interconnected by flexible arms. Additional studies will be required to determine if the native COG within cells is a tightly compacted, bilobed, or a relatively splayed structure.

Effects of COG mutations on its composition and size and on the structure of the Golgi apparatus

The Cog1 and Cog2 proteins were initially identified during the analysis of two classes of CHO cell mutants, ldlB and ldlC (Krieger et al., 1981; Kingsley et al., 1986; Podos et al., 1994; Chatterton et al., 1999). We used immunoblotting of whole cell lysates to determine the steady-state levels of COG subunits in wild-type and mu-

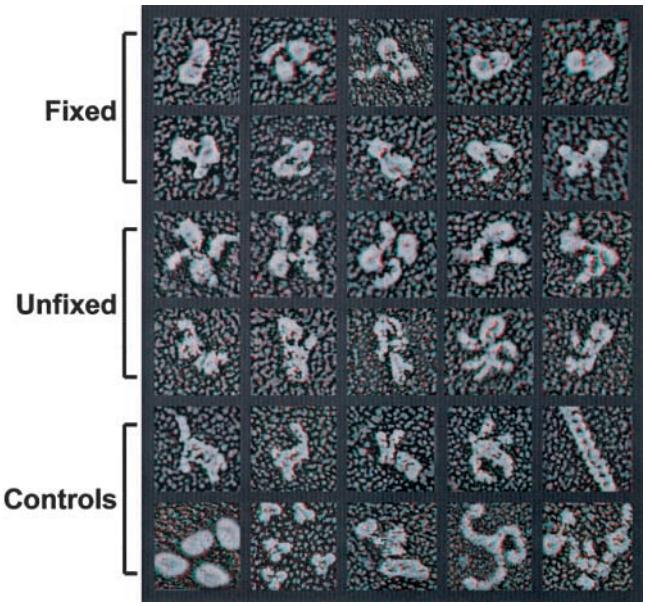

Figure 6. **COG complex architecture**. These anaglyph stereo images are best viewed with red/green stereo glasses (Heuser, 2000). Fixed COG (800 kD, 13S) is in the first and second rows. Unfixed COG is in the third and fourth rows. Fixed mammalian Sec6/8 complex is displayed in the fifth row (Hsu et al., 1998), with F-actin filament in the rightmost panel. Other calibration molecules are in the bottom row (left to right): thyroglobulin (670 kD, 19S), IgG (150 kD), dynactin (1,200 kD; Schafer et al., 1994), clathrin triskelion (630 kD, 7S; Heuser and Kirchhausen, 1985), and cytoplasmic dynein (820 kD, 20S). All panels are 375,000× when viewed as 1-inch squares.

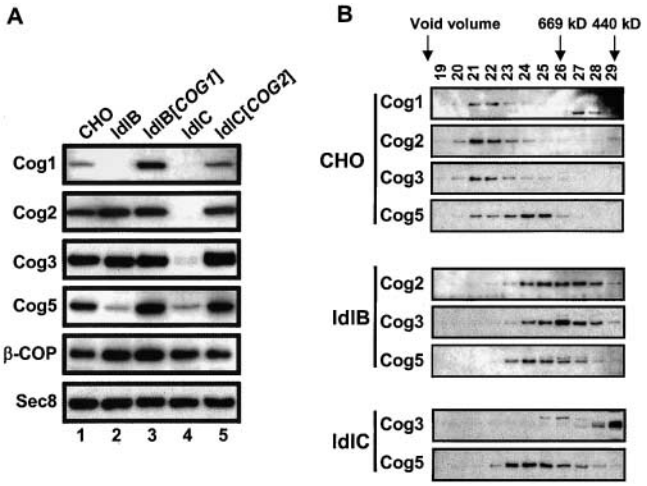

Figure 7. **Steady-state levels of COG components and sizes of complexes in wild-type CHO, ldlB (Cog1), and ldlC (Cog2) cells.** (A) Total cell lysates from the indicated wild-type CHO, ldlB, and ldlC cells, as well as ldlB and ldlC revertants corrected by transfection with the corresponding cDNA expression vectors (ldlB[*COG1*] and ldlC[*COG2*]) were fractionated by 7% SDS-PAGE and immunoblotted with antibodies to the indicated COG subunits or control proteins (β-COP and Sec8). (B) Cytosols from wild-type CHO (top), ldlB (middle), and ldlC (bottom) cells were fractionated by Superose 6 gel filtration chromatography. Samples of the fractions were analyzed by 7% SDS-PAGE and immunoblotted with the indicated antibodies. The position of the void volume and the elution positions of size standards (thyroglobulin, 669 kD; apoferritin, 440 kD) are shown at the top.

tant cells, as well as stable transfectants in which the mutants' phenotypes were corrected by transfection with expression vectors encoding either Cog1 (ldlB[*COG1*]) or Cog2 (ldlC[*COG2*]). Fig. 7 A shows that, as previously described (Podos et al., 1994), Cog2 was not detected in the ldlC mutant (lane 4), whereas a somewhat greater than wild-type expression level of Cog2 was observed in ldlC[*COG2*] cells. Similar results were obtained for Cog1 expression in wild-type (lane 1), ldlB (lane 2), and ldlB[*COG1*] cells (lane 3), as expected from prior studies (Chatterton et al., 1999). In ldlB cells, the level of Cog5 was significantly lower (lane 2) than in the wild-type (lane 1) or transfectant (lane 3) controls, but the levels of Cog3 and Cog2 were not altered. In contrast, the levels in ldlC cells of Cog1, -3, and -5 were dramatically reduced (lane 4) compared with wild-type (lane 1) or transfected (lane 5) controls. The residual level of Cog5 in ldlC cells (lane 4) was similar to that in ldlB cells (lane 2). The absence of Cog1 (lane 2) or Cog2 (lane 4) did not alter the levels of components of two other complexes involved in secretion, β-COP and Sec8 (Fig. 7 A). Thus, the absence of some COG subunits affected the steady-state levels of other COG components, providing genetic evidence for their interactions. The different effects of the absence of Cog1 and Cog2 on the levels of other COG subunits suggest that Cog1 and Cog2 play distinct roles in the organization of the complex.

The absence of one or more subunits in a macromolecular assembly, such as COG, should alter the size of the residual complex. We size fractionated wild-type (Fig. 7 B, top), ldlB (middle), and ldlC (bottom) cytosols and examined the distribution of the Cog1, -2, -3, and -5 subunits by immunoblotting. In wild-type cytosol, Cog1, -2, -3, and -5 comigrated (Fig. 7 B, fractions 21 and 22), and we detected a distinct, smaller complex containing Cog5 but not the other immunodetectable COG components (fractions 23–26, compare with Fig. 3, peak 1). In ldlB (Cog1) cytosol, the other COG subunits were no longer present in the large complex (Fig. 7 B, fractions 21 and 22; Chatterton et al., 1999). Rather, their mobilities showed, in addition to the Cog5 present in the smaller complex (fractions 23–26), that they were components of an even smaller entity whose size was much larger than that expected for the individual subunits. In the ldlC (Cog2) mutant, where the steady-state levels of total cellular Cog3 and Cog5 were significantly reduced (Fig. 7 A), these subunits were no longer found in the large complex (Fig. 7 B, fractions 21 and 22). These data support the conclusion that Cog1, -2, -3, and -5 are components of one large complex. They also show that in CHO cells, as was the case for bovine brain cytosol, some Cog5 was present in a distinct complex that was smaller than COG and did not contain Cog1, -2, and -3. The chromatographic mobility of this smaller Cog5-containing complex was apparently unperturbed by the absence of Cog1 or Cog2.

The disruptions in the size and composition of COG in ldlB and ldlC mutants (Fig. 7) are associated with pleiotropic Golgi functional defects (Kingsley et al., 1986; Podos et al., 1994; Chatterton et al., 1999). Therefore, we examined,

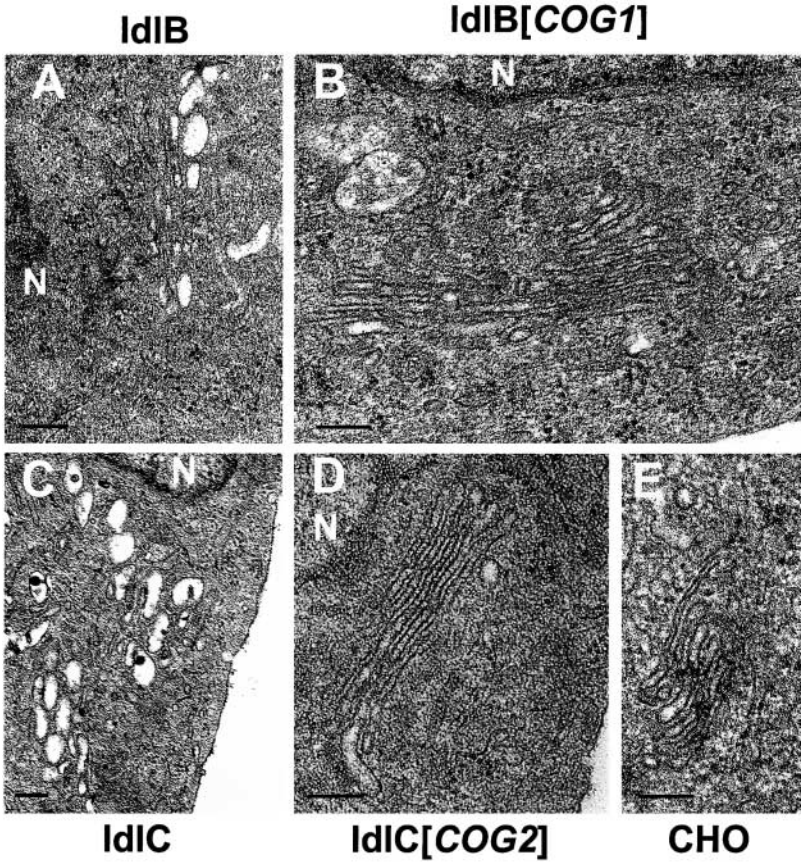

Figure 8. **Ultrastructure of the Golgi apparatus in wild-type, mutant, and revertant cells.** Monolayers of cells were fixed in situ and epon embedded. Thin epon sections (40–50 nm) were viewed by transmission EM as described in the Materials and methods. Juxtanuclear regions with Golgi cisternae are shown: (A) ldlB, (B) ldlB[*COG1*] (mutation complemented by the corresponding cDNA), (C) ldlC, (D) ldlC[*COG2*], and (E) wild-type CHO. N, nucleus. Bars, 200 nm.

by transmission EM, the morphology of the Golgi apparatus in wild-type CHO, ldlB, and ldlC cells and their corresponding phenotypically corrected transfectants (ldlB [*COG*1] and ldlC[*COG2*]). Fig. 8 shows that the Golgi morphology in both ldlB and ldlC mutants was abnormal. At least half, and sometimes all, of the identifiable cisternae were dilated in the mutants. These dilated cisternae were not seen in control wild-type cells or transfectants, suggesting that they were related to the functional defects in ldlB and ldlC mutants. Additional studies will be required to determine if the dilated cisternae are located predominantly on the cis or trans sides of the Golgi stack.

Discussion

The components of the COG complex

We characterized the composition, structure, and function of a mammalian conserved oligomeric Golgi-localized protein complex, the COG complex. Purification of COG and identification of its subunits, Cog1–8, showed that some of its polypeptides are known components of the GTC, the ldlCp complex, and the Sec34 complex (Table II). Coimmunoprecipitation experiments showed that COG components (Cog1, -2, -3, and -5) are physically associated. Furthermore, the steady-state levels of some COG subunits (Cog1, -2, -3, and -5) were dramatically reduced in ldlB (Cog1) or ldlC (Cog2) mutants, establishing genetic associations between them. The loss of Cog1 or Cog2 in the mutants also led to a reduction in the sizes of the residual complexes. In addition, seven COG subunits (Cog1–5, -7, and -8) have been localized to the mammalian Golgi apparatus (Podos et al., 1994; Walter et al., 1998; Suvorova et al., 2001; Whyte and Munro, 2001; this study). Finally, independent analyses of the yeast Sec34/35 complex (Kim et al., 1999, 2001; VanRheenen et al., 1999; Whyte and Munro, 2001; Ram et al., 2002) show that it too is a hetero-octameric complex, and five of its subunits are close homologues of COG subunits (Cog3–6 and -8) (Table II). The remaining three subunits in the COG and Sec34/35 complex are also likely to be related functionally. Indeed, yeast Sec35p and Cog2 have limited sequence similarity (Whyte and Munro, 2001).

The structure of COG

Quick freeze/deep etch/rotary shadow EM suggests that COG, at least after fixation with glutaraldehyde, is ~37 nm long and divided into two almost equally sized lobes (designated A and B, see below). In unfixed specimens, we observed similar bilobed structures and, more frequently, splayed structures with multiple small globular domains connected by relatively flexible extensions (Fig. 6).

Insight into the relationship between the bilobed structure of COG and its subunit composition can be deduced from our studies in combination with studies of the yeast Sec34/35 complex (Fig. 9). During the COG purification, we noted that Cog5 was present both in COG (Fig. 1, peak 2) and in a smaller complex (Fig. 1, peak 1). The smaller complex may represent a fragment of the COG complex (Fig. 9, lobe B; see below), contain COG subunits in addition to Cog5 (see below), and thus correspond to one of the two lobes seen in the EM images. Because Cog1, -2, and -3 are

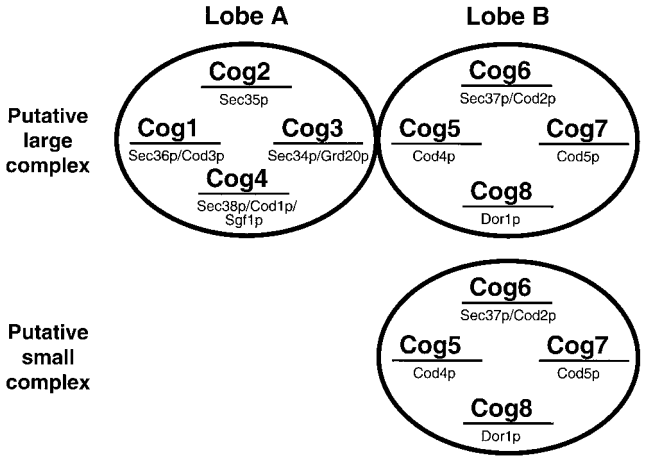

Figure 9. **Schematic representation of the putative bilobed subunit organization of the mammalian (large type) and yeast (small type) COG complexes.**

not part of the Cog5-containing smaller complex, they presumably reside in the other lobe.

Division of COG into two approximately equal-sized lobes, each having four subunits, is consistent with the classification by Whyte and Munro (2001) of the yeast Sec34/35 complex's subunits into two groups of four, based on the severity of their mutant phenotypes. The first group, characterized by more severe phenotypes, contains Sec34p, Sec35p, Cod1p, and Cod3p, whereas the other group, distinguished by weaker phenotypes, comprises Dor1p, Cod2p, Cod4p, and Cod5p (Whyte and Munro, 2001). We suggest that the stronger and weaker phenotypes are the result of mutations in subunits residing in distinct lobes of the complex; mutations in lobe A produce stronger phenotypes (e.g., *sec34*), and those in lobe B (e.g., *cod4*) give weaker ones (Fig. 9).

With this assumption we can assign other subunits to the A and B lobes of COG. The weak phenotype of the *cod4* mutant places Cog5/Cod4p in lobe B and consequently Cog1, -2, and -3, which are in the other lobe, in lobe A (Fig. 9). Moreover, we propose that the fourth protein in lobe A is Cog4/Cod1p because of the severe *cod1* phenotype (Kim et al., 2001; Whyte and Munro, 2001; Ram et al., 2002). Finally, the remaining proteins, Cog6–8, must reside in lobe B (Fig. 9), consistent with the weaker phenotypes of *cod2* and *dor1* mutants (Whyte and Munro, 2001), the yeast counterparts of Cog6 and Cog8. The proposed composition of lobe B is consistent with it potentially representing the smaller Cog5-containing complex in bovine brain and CHO cell cytosols.

As a consequence of these assignments (Fig. 9 and Table IV), we suggest that Cog7 in lobe B is functionally analogous to yeast Cod5p. Lastly, we speculate that (a) Cog2 and yeast Sec35p are functional analogs because of their weak sequence similarities and assignments to the A lobes, and (b) the remaining unpaired subunits, Cog1 and yeast Cod3p in lobe A, are probably functional analogs. (Fig. 9 and Table IV). Supporting this, mammalian Cog2 and Cog3, or the corresponding yeast Sec35p and Sec34p, comigrate at a smaller size when Cog1/Cod3p mutant cytosol is gel filtered (Fig. 7; Ram et al., 2002). Further work will be required to rigorously test this model for COG.

The function of COG

Cog1 and Cog2 were originally identified in a genetic screen for mutants that block LDLR activity in CHO cells (Krieger et al., 1981). Analysis of the transport/secretion of the LDLR and vesicular stomatitis virus (VSV) in ldlB and ldlC mutants and in a revertant of ldlC cells bearing an extragenic suppressor of the LDLR-deficient phenotype (Reddy and Krieger, 1989) strongly suggested that neither membrane protein transport through the secretory pathway nor normal endocytic cycling are disrupted profoundly. The pleiotropic defects in Golgi–associated glycosylation reactions in these mutants resulted in abnormally glycosylated, and consequently unstable, LDLRs. The ldlB and ldlC cells have essentially identical defects in numerous medial- and trans-Golgi–associated reactions that affect virtually all protein- (N-linked and O-linked) and lipid-linked glycoconjugates (Kingsley et al., 1986). The pleiotropic nature of the defects suggested that the mutations might affect the regulation, compartmentalization, transport, or activity of several different Golgi enzymes and/or enzyme substrates, or the internal milieu of the Golgi apparatus. This correlates well with our finding in this study that Golgi cisternae are dilated in these mutants.

Another COG component, Cog5, was first identified (Walter et al., 1998) in an in vitro assay that measures glycosylation of a cargo protein as a consequence of a membrane fusion event (Balch et al., 1984). The assay is dependent on maintenance of an intraluminal environment that is compatible with glycosylation (Hiebsch and Wattenberg, 1992) and on vesicular transport factors, especially those involved

Table IV. **Tentative classification of COG complex subunits into two groups based on biochemical behavior and analogy to yeast phenotypic data**

Group A		Group B	
Mammalian; present exclusively in the large complex (corresponding yeast protein)	**Yeast; stronger phenotype**	**Mammalian; present in both large and small complexes (corresponding yeast protein)**	**Yeast; weaker phenotype**
Cog1 (none)	*cod3*	Cog5 (Cod4p)	*cod4*
Cog2 (none)	*sec35*	Cog6 (Cod2p)	*cod2*
Cog3 (Sec34)	*sec34*	Cog7 (none)	*cod5*
Cog4 (Cod1p)	*cod1*	Cog8 (Dor1p)	*dor1*

Assignments are based on protein purification, chromatography, immunoblotting (this study), and yeast phenotypic data (Whyte and Munro, 2001). Yeast homologues of mammalian proteins are shown in parentheses.

in membrane docking or fusion (Block et al., 1988; Clary and Rothman, 1990; Waters et al., 1992; Legesse-Miller et al., 1998). Although this system was originally thought to measure anterograde vesicle traffic through the Golgi apparatus (Balch et al., 1984), it has been suggested (Love et al., 1998) that it may in fact measure retrograde traffic of the glycosyltransferase to the cargo and, as such, recapitulate retrograde intra-Golgi traffic. The fact that COG is active in this in vitro system suggests that it may act in docking and/or fusion of vesicles within the Golgi apparatus, possibly including retrograde glycosyltransferase-bearing vesicles.

Further insight into COG function can be derived from studies of its yeast homologue, the Sec34/35 complex. *sec34* and *sec35* exhibit slow growth, missorting of proteins in the secretory/vacuolar system, defective protein secretion, underglycosylation of proteins, accumulation of vesicles, and dilated membranous compartments (Wuestehube et al., 1996; Kim et al., 2001). Mutations in Sec34/35 complex subunits genetically interact with mutations in components involved in multiple steps of transport to and through the Golgi apparatus (VanRheenen et al., 1998; Kim et al., 1999, 2001; Spelbrink and Nothwehr, 1999; VanRheenen et al., 1999; Whyte and Munro, 2001; Ram et al., 2002). Of particular note is the recent observation that Sec34/35 complex components, which are located throughout the Golgi apparatus (Kim et al., 2001), show strong genetic interactions with subunits of the COPI vesicle coat (Kim et al., 2001; Ram et al., 2002), which is thought to function in retrograde traffic within the Golgi apparatus and from the Golgi apparatus to the ER (Letourneur et al., 1994). This prompted Ram et al. (2002) to suggest that the Sec34/35 complex may function in retrograde intra-Golgi traffic, a possibility we have independently considered for mammalian COG. Indeed, it is known that maintenance of Golgi enzymes requires their retrograde vesicular transport from distal compartments (Harris and Waters, 1996; Martinez-Menarguez et al., 2001). Thus, a defect in intra-Golgi retrograde traffic could lead to the glycosylation defects seen in mammalian and yeast COG mutants. Compromised COG activity might also contribute to an aberrant Golgi structure through mislocalization of crucial Golgi proteins. In addition, the compromised biosynthetic trafficking seen in some yeast Sec34/35 complex mutants (Wuestehube et al., 1996; Kim et al., 2001) may be a consequence of secondary anterograde trafficking defects arising from primary retrograde trafficking defects (Gaynor and Emr, 1997; Reilly et al., 2001).

Whyte and Munro (2001) suggested that the yeast Sec34/35 complex may be evolutionarily and functionally related to the Sec6/8 complex, also called the exocyst, which has been proposed to tether transport vesicles to the plasma membrane (Grindstaff et al., 1998; Guo et al., 1999). We have found that the mammalian COG and Sec6/8 complexes comigrate during numerous purification steps. Thus, they share many biochemical and biophysical properties, including hydrodynamic size and shape and overall surface charge/hydrophobicity (this study; unpublished data). Also, as noted previously (Walter et al., 1998), both complexes contain eight subunits with very similar molecular weights. However, their appearances in deep etch EM differ. Therefore, further work to elucidate the relationship of these complexes is required.

In summary, mammalian COG and its yeast homologue clearly play important roles in determining the structure and function of the Golgi apparatus and can influence intracellular membrane trafficking. However, their precise mechanism of action remains unknown. This is highlighted by the fact that the yeast Sec34/35 complex's subunits exhibit numerous genetic interactions both with cellular components proposed to be involved in tethering vesicles to the early Golgi apparatus (VanRheenen et al., 1998, 1999; Kim et al., 1999, 2001; Ram et al., 2002) and with the COPI vesicle coat (Kim et al., 2001; Ram et al., 2002). Genetic and biochemical studies raise the possibility that the COG and Sec34/35 complexes may be directly involved in vesicular membrane transport processes (e.g., vesicle budding, targeting, or fusion reactions). Alternatively, COG may indirectly influence trafficking as a consequence of a direct influence on the structure or activity of one or more compartments of the Golgi apparatus (e.g., potential scaffolding activity).

The characterization of the composition and structure of COG combined with the analysis of COG mutants provides a strong foundation for future studies of the function of this important molecular machine.

Materials and methods

Materials

Antibodies used for immunoblotting (IB) and for immunofluorescence (IF) and their dilutions were as follows: rabbit polyclonal affinity-purified anti-Cog5 (anti–GTC-90) (IB, 1:500–1,000; IF, 1:100; Walter et al., 1998), rabbit polyclonal affinity-purified anti-Cog2 Cpep (anti-ldlCp Cpep) (IB, 1:2,000–3,000; Podos et al., 1994), rabbit polyclonal anti-Cog3 serum (anti-hSec34) (IB, 1:10,000; Suvorova et al., 2001), affinity-purified rabbit anti-Cog3 (anti-hSec34) (IB, 1:3,000; IF, 1:3,000; Suvorova et al., 2001), mouse monoclonal anti-Cog1 (anti-ldlBp) (IB, 1:250–600; IF, 1:100; BD Biosciences), rabbit polyclonal anti-Cog1 (anti-ldlBp) antiserum (IB, 1:3,000), affinity-purified rabbit polyclonal anti-Cog1 (anti-ldlBp) (IF, 1:150), mouse monoclonal anti-Sec8 (IB, 1:2,500; BD Biosciences), mouse monoclonal anti–β-COP (IB, 1:1,000; Sigma-Aldrich), rabbit anti–mannosidase II (IF, 1:2,000; a gift from Kelley Moremen, University of Georgia, Athens, GA), and mouse monoclonal anti–HA-11 (IF, 1:400; Covance).

Dialysis membranes (mol wt cutoff of 12–14 kD) were from BioDesign Inc. The ceramic hydroxyapatite column was from Bio-Rad Laboratories, and all other chromatography materials and secondary antibodies conjugated with HRP for immunoblotting and chemiluminescence were obtained from Amersham Pharmacia Biotech. Compactin was a gift from A. Endo (Tokyo Nodo University, Tokyo, Japan). Newborn calf lipoprotein-deficient serum (NCLPDS) and LDL were prepared as previously described (Krieger, 1983). Glutaraldehyde, osmium tetroxide, uranyl acetate, and eponate were obtained from Ted Pella Inc. All other chemicals were purchased from Sigma-Aldrich, unless otherwise noted.

Purification of COG

All procedures were performed at 4°C. Solutions were buffered with 25 mM TrisCl, pH 8.0, 1 mM DTT (TD) and contained the indicated amounts of KCl (e.g., TD + 1 M KCl) and glycerol, unless otherwise noted. Bovine brain cytosol was ammonium sulfate precipitated as previously described (Waters et al., 1992). After resuspension of the precipitated proteins and adjustment of the salt concentration to 1M KCl, the sample was chromatographed on butyl-Sepharose. The COG complex was eluted with TD + 10 mM KCl, concentrated, and the concentration of KCl in the TD buffer was adjusted to 160 mM KCl by dialysis and the addition of salt. The sample was then applied to a MonoQ HR10/10 column, COG eluted in a KCl gradient and dialyzed overnight against 25 mM Hepes-KOH, pH 7.0, 100 mM KCl, 10% glycerol. After adding potassium phosphate (KP_i) to a final con-

centration of 5 mM, the dialyzed sample was chromatographed on a ceramic hydroxyapatite column. COG complex was eluted with a KP_i gradient and fractions were immediately dialyzed against TD + 100 mM KCl, 10% glycerol in a microdialyzer (GIBCO BRL). The second peak of Cog5 immunoreactivity (Fig. 1 A, peak 2) was then concentrated and loaded onto a Superose 6 HR10/30 sizing column. Fractions containing COG complex were pooled and chromatographed on a MiniQ column. An estimated 70 μg of COG complex eluted at ~220 mM KCl in the gradient.

Analytical gel filtration of the two different Cog5-containing complexes (Fig. 1 B) was performed on a Superose 6 3.2/30 column.

Gel filtration chromatography of COG complex in cell lysates from CHO cell lines (Fig. 7 B) was performed as previously described (Chatterton et al., 1999).

Mass spectrometry

COG complex (~40 μg) was separated on a 1-mm-thick 7.5% SDS-polyacrylamide gel. The gel was stained with colloidal Coomassie blue (Invitrogen) and destained in water. Four individual bands and two doublets were excised and subjected to electrospray MS/MS peptide sequencing after in-gel trypsin digestion and HPLC separation (Yates et al., 1999) at the Harvard Microchemistry Facility.

Deep etch EM of purified COG complex

To visualize single COG complex particles, ~20 μg of purified COG complex (Fig. 2 A, fraction 18) was visualized on mica by quick freeze/deep etch/rotary shadowing microscopy as previously described (Heuser, 1983). For glutaraldehyde fixation, the 10 μg/ml COG solution was mixed with a small volume of 7% glutaraldehyde and incubated for 30 s before mixing with a suspension of mica flakes. Final anaglyph 3-D images were generated as described by Heuser (2000).

Transmission EM of cells

Cells were rapidly rinsed with PBS containing 1 mM $MgCl_2$ and 0.1 mM $CaCl_2$, fixed with 2% glutaraldehyde in 0.1 M sodium cacodylate-HCl, pH 7.2, for 60 min at 4°C, and postfixed with 2% osmium tetraoxide in 0.1 M sodium cacodylate-HCl for 60 min at 4°C. The cells were harvested by scraping from the plastic dish and centrifugation at 750 *g* for 5 min to form a small pellet. The pellet was then dehydrated in graded alcohol up to 70% and en block stained with 70% alcoholic uranyl acetate for 30 min at 4°C. The samples were then processed for epon embedding (Vasile et al., 1983). Thin epon sections were poststained with uranyl acetate and Reynold's lead citrate and viewed with a Philips 400 electron microscope operated at 80 kV.

Immunoprecipitation of the COG complex from rat liver cytosol and a partially purified bovine brain COG complex preparation

For immunoprecipitation, 5 μg of monoclonal anti-Cog1 antibody was added to 50 μl of partially purified bovine brain COG complex (purified through the MonoQ step). For immunoprecipitation with affinity-purified anti-Cog2 antibody, 5 μg of antibody with or without antigenic peptide (see below) was added to 400 μg of rat liver cytosol. The samples were adjusted to a total of 500 μl with PBS with (for anti-Cog1) or without (for anti-Cog2) 5% (wt/vol) nonfat dried milk and incubated overnight at 4°C. Subsequently, the sample was incubated for 2 h at room temperature with 10 μl of a 50% (vol/vol) slurry of protein A–Sepharose CL-4B in PBS. The beads were then washed four times with 500 μl PBS with (for anti-Cog1) or without (for anti-Cog2) 5% (wt/vol) nonfat dried milk and once with 500 μl of PBS. Precipitated proteins were eluted in SDS sample buffer and analyzed by immunoblotting. For anti-Cog2 antigenic peptide competition, the anti-Cog2 antibody was preincubated for 1 h at room temperature with 10 μg of the COOH-terminal antigenic peptide (Cpep; Podos et al., 1994) in 100 μl of PBS before addition to the cytosol.

Preparation of the pHM6-Cog7 expression plasmid

Full length Cog7 cDNA was cloned into the pHM6 vector (Roche) with the restriction enzymes HindIII and KpnI, resulting in the plasmid pHM6-Cog7 coding for an HA epitope–tagged Cog7.

Mammalian cell culture and transfection

Wild-type CHO, ldlB, ldlC, ldlB[*COG1*], and ldlC[*COG2*] cells were grown at 37°C in plastic culture dishes as previously described (Podos et al., 1994; Chatterton et al., 1999). Here we have renamed two stably transfected cell lines to conform to the nomenclature introduced in this paper (ldlBp is Cog1; ldlCp is Cog2) as follows: ldlB[*LDLB*] cells (Chatterton et al., 1999) are now called ldlB[*COG1*] cells and ldlC[*LDLC*] cells (Podos et al., 1994) are called ldlC[*COG2*] cells. HeLa cells for immunofluorescence were grown in standard medium on coverslips and transfected with the calcium phosphate method (Ausubel et al., 1995).

Immunofluorescence microscopy

Cells grown on coverslips were processed at room temperature as follows. Cells were washed once with PBS and fixed by rinsing and incubating for 25 min with 2% paraformaldehyde (EM Sciences) in 0.1 M NaP_i, pH 7.2. The coverslips were then rinsed twice and incubated for 15 min in 0.1 M glycine in PBS. Cells were then blocked in P-B (0.1% saponin, 1% BSA, 2% normal goat serum [Chemicon]) for 30 min. The coverslips were washed with PBS followed by a 5-min treatment with 6 M urea in PBS, four 5-min washes in PBS, and an additional 45-min incubation in P-B. The treatment with urea was omitted in the case of double staining with anti–mannosidase II and anti-HA antibodies. The cells were then incubated for 1 h with primary antibodies and washed with P-B four times for 5 min each. Secondary antibodies (Alexa®488 goat anti–rabbit IgG [H+L] conjugate and Alexa®546 or Alexa®568 goat anti–mouse IgG [H+L] conjugate [Molecular Probes]) diluted 1:750 in P-B were applied for 1 h, and the coverslips were washed with PBS eight times for 5 min and with water for 5 min. Images were obtained with a ZEISS LSM 510 laser confocal microscope.

Online supplemental material

For a more detailed description of several methods and the generation of the anti-Cog1 and anti-Cog2 polyclonal antibodies, see the supplemental materials located at http://www.jcb.org/cgi/content/full/jcb.200202016/DC1.

We are grateful to Sean Munro (Medical Research Council, Cambridge, UK), Rachna Ram (MIT), and Chris Kaiser (MIT) for communicating unpublished results and cooperating in naming the complex, Sandy Schmid (Scripps Research Institute, La Jolla, CA) for encouragement and support, and Sarah Richman (Princeton University) for the first hint that Sec34/35 and COG are homologous. We thank the Harvard Microchemistry Facility for expert mass spectrometry and Joe Goodhouse (Princeton University) and H.R. Horvitz (MIT) for help with confocal fluorescence microscopy. We are grateful to Kelley Moremen and Juan Bonifacino (National Institutes of Health, Bethesda, MD) for providing antibodies.

This work was supported by the National Institutes of Health (GM59280 to M.G. Waters, GM59115 to M. Krieger, and GM29647 to J.E. Heuser).

Submitted: 5 February 2002
Revised: 18 March 2002
Accepted: 21 March 2002

References

Ausubel, F.M., R. Brent, R.E. Kingston, D.D. Moore, J.G. Seidman, J.A. Smith, and K. Struhl. 1995. Short Protocols in Molecular Biology. John Wiley & Sons, Inc., New York. 910 pp.

Balch, W.E., W.G. Dunphy, W.A. Braell, and J.E. Rothman. 1984. Reconstitution of the transport of protein between successive compartments of the Golgi measured by the coupled incorporation of *N*-acetylglucosamine. *Cell.* 39:405–416.

Berger, B., D.B. Wilson, E. Wolf, T. Tonchev, M. Milla, and P.S. Kim. 1995. Predicting coiled coils by use of pairwise residue correlations. *Proc. Natl. Acad. Sci. USA.* 92:8259–8263.

Block, M.R., B.S. Glick, C.A. Wilcox, F.T. Wieland, and J.E. Rothman. 1988. Purification of an *N*-ethylmaleimide-sensitive protein catalyzing vesicular transport. *Proc. Natl. Acad. Sci. USA.* 85:7852–7856.

Bonfanti, L., A.A. Mironov, Jr., J.A. Martinez-Menarguez, O. Martella, A. Fusella, M. Baldassarre, R. Buccione, H.J. Geuze, A.A. Mironov, and A. Luini. 1998. Procollagen traverses the Golgi stack without leaving the lumen of cisternae: evidence for cisternal maturation. *Cell.* 95:993–1003.

Chatterton, J.E., D. Hirsch, J.J. Schwartz, P.E. Bickel, R.D. Rosenberg, H.F. Lodish, and M. Krieger. 1999. Expression cloning of LDLB, a gene essential for normal Golgi function and assembly of the ldlCp complex. *Proc. Natl. Acad. Sci. USA.* 96:915–920.

Clary, D.O., and J.E. Rothman. 1990. Purification of three related peripheral membrane proteins needed for vesicular transport. *J. Biol. Chem.* 265:10109–10117.

Gaynor, E.C., and S.D. Emr. 1997. COPI-independent anterograde transport: cargo-selective ER to Golgi protein transport in yeast COPI mutants. *J. Cell Biol.* 136:789–802.

Grindstaff, K.K., C. Yeaman, N. Anandasabapathy, S.C. Hsu, E. Rodriguez-Boulan, R.H. Scheller, and W.J. Nelson. 1998. Sec6/8 complex is recruited to cell-cell contacts and specifies transport vesicle delivery to the basal-lateral

membrane in epithelial cells. *Cell.* 93:731–740.

Guo, W., D. Roth, C. Walch-Solimena, and P. Novick. 1999. The exocyst is an effector for Sec4p, targeting secretory vesicles to sites of exocytosis. *EMBO J.* 18:1071–1080.

Harris, S.L., and M.G. Waters. 1996. Localization of a yeast early Golgi mannosyltransferase, Och1p, involves retrograde transport. *J. Cell Biol.* 132:985–998.

Heuser, J. 1989. Protocol for 3-D visualization of molecules on mica via the quick-freeze, deep-etch technique. *J. Electron Microsc. Tech.* 13:244–263.

Heuser, J. 2000. How to convert a traditional electron microscopy laboratory to digital imaging: follow the 'middle road.' *Traffic.* 1:614–621.

Heuser, J.E. 1983. Procedure for freeze-drying molecules adsorbed to mica flakes. *J. Mol. Biol.* 169:155–195.

Heuser, J., and T. Kirchhausen. 1985. Deep-etch views of clathrin assemblies. *J. Ultrastruct. Res.* 92:1–27.

Hiebsch, R.R., and B.W. Wattenberg. 1992. Vesicle fusion in protein transport through the Golgi in vitro does not involve long-lived prefusion intermediates. A reassessment of the kinetics of transport as measured by glycosylation. *Biochemistry.* 31:6111–6118.

Hsu, S.C., C.D. Hazuka, R. Roth, D.L. Foletti, J. Heuser, and R.H. Scheller. 1998. Subunit composition, protein interactions, and structures of the mammalian brain sec6/8 complex and septin filaments. *Neuron.* 20:1111–1122.

Hsu, S.C., A.E. Ting, C.D. Hazuka, S. Davanger, J.W. Kenny, Y. Kee, and R.H. Scheller. 1996. The mammalian brain rsec6/8 complex. *Neuron.* 17:1209–1219.

Kim, D.W., M. Sacher, A. Scarpa, A.M. Quinn, and S. Ferro-Novick. 1999. High-copy suppressor analysis reveals a physical interaction between Sec34p and Sec35p, a protein implicated in vesicle docking. *Mol. Biol. Cell.* 10:3317–3329.

Kim, D.-W., T. Massey, M. Sacher, M. Pypaert, and S. Ferro-Novick. 2001. Sgf1p, a new component of the Sec34p/Sec35p complex. *Traffic.* 2:820–830.

Kingsley, D.M., and M. Krieger. 1984. Receptor-mediated endocytosis of low density lipoprotein: somatic cell mutants define multiple genes required for expression of surface-receptor activity. *Proc. Natl. Acad. Sci. USA.* 81:5454–5458.

Kingsley, D.M., K.F. Kozarsky, M. Segal, and M. Krieger. 1986. Three types of low-density lipoprotein receptor-deficient mutants have pleiotropic defects in the synthesis of N-linked, O-linked, and lipid-linked carbohydrate chains. *J. Cell Biol.* 102:1576–1585.

Krieger, M. 1983. Complementation of mutations in the LDL pathway of receptor-mediated endocytosis by cocultivation of LDL receptor-defective hamster cell mutants. *Cell.* 33:413–422.

Krieger, M., M.S. Brown, and J.L. Goldstein. 1981. Isolation of Chinese hamster cell mutants defective in the receptor-mediated endocytosis of low density lipoprotein. *J. Mol. Biol.* 150:167–184.

Legesse-Miller, A., Y. Sagiv, A. Porat, and Z. Elazar. 1998. Isolation and characterization of a novel low molecular weight protein involved in intra-Golgi traffic. *J. Biol. Chem.* 273:3105–3109.

Letourneur, F., E.C. Gaynor, S. Hennecke, C. Demolliere, R. Duden, S.D. Emr, H. Riezman, and P. Cosson. 1994. Coatomer is essential for retrieval of dilysine-tagged proteins to the endoplasmic reticulum. *Cell.* 79:1199–1207.

Love, H.D., C.-C. Lin, C.S. Short, and J. Ostermann. 1998. Isolation of functional Golgi-derived vesicles with a possible role in retrograde transport. *J.Cell Biol.* 140:541–551.

Martinez-Menarguez, J.A., R. Prekeris, V.M. Oorschot, R. Scheller, J.W. Slot, H.J. Geuze, and J. Klumperman. 2001. Peri-Golgi vesicles contain retrograde but not anterograde proteins consistent with the cisternal progression model of intra-Golgi transport. *J. Cell Biol.* 155:1213–1224.

Mellman, I., and G. Warren. 2000. The road taken: past and future foundations of membrane traffic. *Cell.* 100:99–112.

Mironov, A.A., G.V. Beznoussenko, P. Nicoziani, O. Martella, A. Trucco, H.S. Kweon, D. Di Giandomenico, R.S. Polishchuk, A. Fusella, P. Lupetti, et al. 2001. Small cargo proteins and large aggregates can traverse the Golgi by a common mechanism without leaving the lumen of cisternae. *J. Cell Biol.* 155:1225–1238.

Pelham, H.R., and J.E. Rothman. 2000. The debate about transport in the Golgi—two sides of the same coin? *Cell.* 102:713–719.

Podos, S.D., P. Reddy, J. Ashkenas, and M. Krieger. 1994. LDLC encodes a brefeldin A-sensitive, peripheral Golgi protein required for normal Golgi function. *J. Cell Biol.* 127:679–691.

Ram, R.J., B. Li, and C.A. Kaiser. 2002. Identification of Sec36p, Sec37p and Sec38p: components of the yeast complex that contains Sec34p and Sec35p. (February 28, 2002) *Mol. Biol. Cell.* 10.1091/mbc.01-10-0495.

Reddy, P., and M. Krieger. 1989. Isolation and characterization of an extragenic suppressor of the low-density lipoprotein receptor-deficient phenotype of a Chinese hamster ovary cell mutant. *Mol. Cell. Biol.* 9:4799–4806.

Reilly, B.A., B.A. Kraynack, S.M. VanRheenen, and M.G. Waters. 2001. Golgi-to-endoplasmic reticulum (ER) retrograde traffic in yeast requires Dsl1p, a component of the ER target site that interacts with a COPI coat subunit. *Mol. Biol. Cell.* 12:3783–3796.

Rothman, J.E. 1994. Mechanisms of intracellular protein transport. *Nature.* 372:55–63.

Sacher, M., J. Barrowman, W. Wang, J. Horecka, Y. Zhang, M. Pypaert, and S. Ferro-Novick. 2001. TRAPP I implicated in the specificity of tethering in ER-to-Golgi transport. *Mol. Cell.* 7:433–442.

Schafer, D.A., S.R. Gill, J.A. Cooper, J.E. Heuser, and T.A. Schroer. 1994. Ultrastructural analysis of the dynactin complex: an actin-related protein is a component of a filament that resembles F-actin. *J. Cell Biol.* 126:403–412.

Spelbrink, R.G., and S.F. Nothwehr. 1999. The yeast *GRD20* gene is required for protein sorting in the trans-Golgi network/endosomal system and for polarization of the actin cytoskeleton. *Mol. Biol. Cell.* 10:4263–4281.

Suvorova, E.S., R.C. Kurten, and V.V. Lupashin. 2001. Identification of a human orthologue of Sec34p as a component of the cis-Golgi vesicle tethering machinery. *J. Biol. Chem.* 276:22810–22818.

VanRheenen, S.M., X. Cao, V.V. Lupashin, C. Barlowe, and M.G. Waters. 1998. Sec35p, a novel peripheral membrane protein, is required for ER to Golgi vesicle docking. *J. Cell Biol.* 141:1107–1119.

VanRheenen, S.M., X. Cao, S.K. Sapperstein, E.C. Chiang, V.V. Lupashin, C. Barlowe, and M.G. Waters. 1999. Sec34p and Sec35p are components of a protein complex required for vesicle tethering the yeast Golgi. *J. Cell Biol.* 147:729–742.

Vasile, E., M. Simionescu, and N. Simionescu. 1983. Visualization of the binding, endocytosis, and transcytosis of low-density lipoprotein in the arterial endothelium in situ. *J. Cell Biol.* 96:1677–1689.

Walter, D.M., K.S. Paul, and M.G. Waters. 1998. Purification and characterization of a novel 13 S hetero-oligomeric protein complex that stimulates in vitro Golgi transport. *J. Biol. Chem.* 273:29565–29576.

Waters, M.G., D.O. Clary, and J.E. Rothman. 1992. A novel 115-kD peripheral membrane protein is required for intercisternal transport in the Golgi stack. *J. Cell Biol.* 118:1015–1026.

Whyte, J.R.C., and S. Munro. 2001. The Sec34/35 Golgi transport complex is related to the exocyst, defining a family of complexes involved in multiple steps of membrane traffic. *Dev. Cell.* 1:527–537.

Wuestehube, L.J., R. Duden, A. Eun, S. Hamamoto, P. Korn, R. Ram, and R. Schekman. 1996. New mutants of *Saccharomyces cerevisiae* affected in the transport of proteins from the endoplasmic reticulum to the Golgi complex. *Genetics.* 142:393–406.

Yates, J.R., III, E. Carmack, L. Hays, A.J. Link, and J.K. Eng. 1999. Automated protein identification using microcolumn liquid chromatography-tandem mass spectrometry. *Methods Mol. Biol.* 112:553–569.